J|A|C|S ARTICLES

Published on Web 12/07/2009

Activatable Magnetic Resonance Imaging Agents for Myeloperoxidase Sensing: Mechanism of Activation, Stability, and Toxicity

Elisenda Rodríguez,[†] Mark Nilges,[‡] Ralph Weissleder,[†,§] and John W. Chen*[,†,§]

Center for Molecular Imaging Research, Department of Radiology, Massachusetts General Hospital, Boston, Massachusetts 02114, Illinois EPR Research Center, University of Illinois, Urbana, Illinois 61801, and Center for Systems Biology, Massachusetts General Hospital, Boston, Massachusetts 02114

Received June 30, 2009; E-mail: jwchen@mgh.harvard.edu

Abstract: Myeloperoxidase (MPO) is increasingly being recognized as an important factor in many inflammatory diseases, particularly cardiovascular and neurological diseases. MPO-specific imaging agents would thus be highly useful to diagnose early disease, monitor disease progression, and quantify treatment effects. This study reports in vitro and in vivo characterizations of the mechanism of interaction between MPO and paramagnetic enzyme substrates based on physical and biological measurements. We show that these agents are activated through a radical mechanism, which can combine to form oligomers and, in the presence of tyrosine-containing peptide, bind to proteins. We further identified two new imaging agents, which represent the near extremes in either oligomerization (mono-5HT-DTPA-Gd) or protein-binding in their activation mechanism (bis-*o*-dianisidine-DTPA-Gd). On the other hand, we found that the agent bis-5HT-DTPA-Gd utilizes both mechanisms when activated. These properties yield distinct in vivo pharmacokinetics profiles for each of these agents that may be exploited for different applications. Specificity studies show that only MPO, but not eosinophil peroxidase, can highly activate these agents, and that MPO activity as low as 0.005 U/mg of tissue can be detected. Gd kinetic lability and cytotoxicity studies further confirm stability of the Gd ion and low toxicity for the 5HT-based agents, suggesting that these agents are suitable for translational in vivo studies.

Introduction

Myeloperoxidase (MPO) is a key enzyme in inflammation.[1] It is the most abundant protein of the azurophilic granules of neutrophils[1] and is also found in monocytes,[2] macrophages,[3] microglia,[4] Kupffer cells,[5] and neurons.[6] MPO contributes to the host immune defense system by generating potent bactericidal oxidants. Besides its physiological role in host defense, MPO and its products have been found and implicated in numerous diseases including atherosclerosis,[7] vasculitis,[8] stroke,[9] cancer,[10] Parkinson's disease,[11] Alzheimer's disease,[6] and multiple sclerosis.[12,13] Clinical trials have shown that MPO levels can be used to predict patient outcome in myocardial infarction[14] and in apparently normal patients,[15] and certain genotypes in the MPO polymorphism are associated with increased disease severity.[16] MPO-deficient individuals have been found to be less susceptible to cardiovascular diseases.[17] Therefore, MPO is emerging to be an important biomarker for many diseases.

[†] Department of Radiology, Massachusetts General Hospital.
[‡] University of Illinois.
[§] Center for Systems Biology, Massachusetts General Hospital.

(1) Klebanoff, S. J. *J. Leukoc. Biol.* **2005**, *77*, 598–625.
(2) Nichols, B. A.; Bainton, D. F. *Lab Invest.* **1973**, *29*, 27–40.
(3) Sugiyama, S.; Okada, Y.; Sukhova, G. K.; Virmani, R.; Heinecke, J. W.; Libby, P. *Am. J. Pathol.* **2001**, *158*, 879–91.
(4) Gray, E.; Thomas, T. L.; Betmouni, S.; Scolding, N.; Love, S. *Brain Pathol.* **2008**, *18*, 86–95.
(5) Brown, K. E.; Brunt, E. M.; Heinecke, J. W. *Am. J. Pathol.* **2001**, *159*, 2081–8.
(6) Green, P. S.; Mendez, A. J.; Jacob, J. S.; Crowley, J. R.; Growdon, W.; Hyman, B. T.; Heinecke, J. W. *J. Neurochem.* **2004**, *90*, 724–33.
(7) Zhang, R.; Brennan, M. L.; Fu, X.; Aviles, R. J.; Pearce, G. L.; Penn, M. S.; Topol, E. J.; Sprecher, D. L.; Hazen, S. L. *JAMA, J. Am. Med. Assoc.* **2001**, *286*, 2136–42.
(8) Ishida-Okawara, A.; Oharaseki, T.; Takahashi, K.; Hashimoto, Y.; Aratani, Y.; Koyama, H.; Maeda, N.; Naoe, S.; Suzuki, K. *Inflammation* **2001**, *25*, 381–7.
(9) Re, G.; Azzimondi, G.; Lanzarini, C.; Bassein, L.; Vaona, I.; Guarnieri, C. *Eur. J. Emerg. Med.* **1997**, *4*, 5–9.
(10) Trush, A.; Esterline, R. L.; Mallet, W. G.; Mosebrook, D. R.; Twerdok, L. E. *Adv. Exp. Med. Biol.* **1991**, *283*, 399–401.
(11) Choi, D. K.; Pennathur, S.; Perier, C.; Tieu, K.; Teismann, P.; Wu, D. C.; Jackson-Lewis, V.; Vila, M.; Vonsattel, J. P.; Heinecke, J. W.; Przedborski, S. *J. Neurosci.* **2005**, *25*, 6594–600.
(12) Hoy, A.; Leininger-Muller, B.; Kutter, D.; Siest, G.; Visvikis, S. *Clin. Chem. Lab. Med.* **2002**, *40*, 2–8.
(13) Nagra, R. M.; Becher, B.; Tourtellotte, W. W.; Antel, J. P.; Gold, D.; Paladino, T.; Smith, R. A.; Nelson, J. R.; Reynolds, W. F. *J. Neuroimmunol.* **1997**, *78*, 97–107.
(14) Brennan, M. L.; Penn, M. S.; Van Lente, F.; Nambi, V.; Shishehbor, M. H.; Aviles, R. J.; Goormastic, M.; Pepoy, M. L.; McErlean, E. S.; Topol, E. J.; Nissen, S. E.; Hazen, S. L. *N. Engl. J. Med.* **2003**, *349*, 1595–604.
(15) Meuwese, M. C.; Stroes, E. S.; Hazen, S. L.; van Miert, J. N.; Kuivenhoven, J. A.; Schaub, R. G.; Wareham, N. J.; Luben, R.; Kastelein, J. J.; Khaw, K. T.; Boekholdt, S. M. *J. Am. Coll. Cardiol.* **2007**, *50*, 159–65.
(16) Nikpoor, B.; Turecki, G.; Fournier, C.; Theroux, P.; Rouleau, G. A. *Am. Heart J.* **2001**, *142*, 336–9.
(17) Kutter, D.; Devaquet, P.; Vanderstocken, G.; Paulus, J. M.; Marchal, V.; Gothot, A. *Acta Haematol.* **2000**, *104*, 10–5.

 10.1021/ja905274f

We have previously reported a prototype activatable MPO-specific MR imaging agent, bis-5HT-DTPA-Gd (DTPA = diethylene triamine pentaacetic acid), and have studied its use in murine models of myocardial infarction, multiple sclerosis, and stroke to report on and track MPO activity in vivo.[18−20] Further rational optimization and translation to higher animals and humans of this class of imaging agents require a deeper understanding of the activation mechanism, interaction with endogenous biomolecules, and potential stability and toxicity issues. In this study, we systematically evaluated this class of agents through chemical modifications with different characteristics and sensitivity to MPO activity. We identified two new agents that are capable of achieving high degree of activation in vitro and in vivo, each with a unique profile that may allow them to be used in different in vitro and in vivo applications. We also present direct evidence that details the mechanism of these agents to explain their behavior in vivo. Furthermore, to better understand the in vivo effects of this class of potentially clinically useful agents, we assessed both the Gd kinetic lability and performed cytotoxicity studies.

Materials and Methods

All of the chemicals required for this work were obtained from Sigma Chemical Co. unless otherwise stated (St. Louis, MO). 5-Hydroxytryptamine was obtained from Alfa Aesar (Ward Hill, MA). DTPA-Gd was purchased as Magnevist from Berlex Inc. (Montville, NJ). Myeloperoxidase and eosinophil peroxidase were obtained from Lee Biosolutions (St. Louis, MO). RAW 264.7 and NIH 3T3 cell lines were obtained from American Type Culture Collection (Manassas, VA). Dulbecco's modified Eagle's medium (DMEM), penicillin/streptomycin, fetal bovine serum (FBS), and the other materials for culturing of cells were purchased from Fisher Scientific (Pittsburgh, PA).

Synthesis of the Chelates Mono-5HT-hydroxytryptamide-DTPA (Mono-5HT-DTPA), Bis-5HT-hydroxytryptamide-DTPA (Bis-5HT-DTPA), Bis-4-aminophenol-DTPA, and Bis-*o*-phenylenediamide-DTPA (Bis-*o*-dianisidine-DTPA). The chelates were synthesized using a modified protocol:[21] 100 mg (0.28 mmol) of DTPA-bisanhydride was reacted with the corresponding amines in DMF (4 mL) in the presence of 100 μL (1 mmol) of pyridine. To get the bis- or the mono-aminosubstituted chelates, the ratio used between the base substrates (5-hydroxytrytamine (5HT), *o*-dianisidine, and 4-aminophenol) and the DTPA-bisanhydride was 0.25 for the mono- and 2.2 for the bis-substituted chelates. To avoid amine oxidation, 50 mg (2.8 mmol) of ascorbic acid was added. The mixture was stirred for 30 min at room temperature. The crude product was first precipitated with ether, dissolved in water, and passed through a C18 cartridge with water and acetonitrile mixtures. The products were purified using HPLC (water/acetonitrile), and peaks were detected at 280 nm. The purity was confirmed by ^{1}H NMR. ^{1}H NMR (400 MHz, D_2O) (see Supporting Information Figure SI1): mono-5HT-DTPA, 7.35 (d, 1H, J = 8.4 Hz), 7.22 (s, 1H), 7.09 (s, 1H), 6.80 (d, 1H, J = 12 Hz), 3.87 (s, 4H), 3.80 (s, 2H), 3.67 (s, 2H), 3.59 (t, 2H, J = 5.6 Hz), 3.46 (s, 2H), 3.29 (t, 2H, J = 6 Hz), 2.93 (m, 6H), 2.88 (m, 2H), 2.84 (m, 2H); bis-5HT-DTPA, 7.32 (d, 2H, J = 8.4 Hz), 7.16 (s, 2H), 7.04 (s, 2H), 6.79 (d, 2H, J = 8.4 Hz), 3.55 (s, 6H), 3.50 (s_{wide}, 4H), 3.41 (s, 6H), 3.25 (s, 2H), 2.89 (s_{wide}, 4H), 2.82 (s_{wide}, 4H), 2.57 (m, 4H); bis-4-aminophenol-DTPA, 7.21 (d, 4H, J = 8.4 Hz), 6.81 (d, 4H, J = 8.4 Hz), 4.01 (s, 4H), 3.85 (m, 8H), 3.45 (m, 4H), 3.37 (m, 4H); bis-*o*-dianisidine-DTPA, 7.66 (d, 2H, J = 8 Hz), 7.92 (d, 2H, J = 8 Hz), 7.07 (m, 4H), 6.96 (m, 4H), 3.96 (s, 8H), 3.86 (s, 10H), 3.79 (m, 8H), 3.52 (s_{wide}, 5H), 3.88 (s_{wide}, 5H). MS (see Supporting Information Figure SI2): *m*/*z* expected mono-5HT-DTPA ($C_{24}H_{33}N_5O_{10}$ + H)$^+$ 552.22, found 552.80; *m*/*z* expected bis-5HT-DTPA ($C_{34}H_{43}N_7O_{10}$ + H)$^+$ 710.31, found 710.32; *m*/*z* expected bis-4-aminophenol-DTPA ($C_{26}H_{33}N_5O_{10}$ + H)$^+$ 576.22, found 576.23; and *m*/*z* expected bis-*o*-dianisidine-DTPA ($C_{42}H_{51}N_7O_{12}$ + H)$^+$ 846.36, found, 846.70.

Synthesis of the Imaging Agents Mono-5HT-DTP-Gd, Bis-5HT-DTPA-Gd, Bis-4-aminophenol-DTPA-Gd, and Bis-*o*-dianisidine-DTPA-Gd. The synthesis of corresponding Gd^{3+} imaging agents was performed in a 5% citric acid solution (pH = 5.0) at room temperature. $GdCl_3 \cdot 6H_2O$ was used in 1.5-fold excess in comparison to the chelates, and the reaction was stirred for 1 h. Final products were purified using HPLC with water and acetonitrile, and peaks were detected at 280 nm. The purity of the resultant imaging agents was measured by analytical HPLC that showed >96% purity for all imaging agents (see Supporting Information Figure SI3). MS (see Supporting Information Figure SI4): *m*/*z* expected mono-5HT-DTPA-Gd ($C_{34}H_{38}N_7O_{10}Gd$ + H)$^+$ 707.22, found 707.33; *m*/*z* expected bis-5HT-DTPA-Gd ($C_{34}H_{40}N_7O_{10}Gd$ + H)$^+$ 865.21, found 865.4; *m*/*z* expected bis-4-aminophenol-DTPA-Gd ($C_{26}H_{30}N_5O_{10}Gd$ + H)$^+$ 731.22, found 731.6; and *m*/*z* expected bis-*o*-dianisidine-DTPA-Gd ($C_{42}H_{48}N_7O_{12}Gd$ + H)$^+$ 1001.36, found 1001.50.

ICP-AES Measurements. To compute the relaxivity for each imaging agent, the Gd^{3+} concentration was determinated by inductively coupled plasma atomic emission spectroscopy (ICP-AES) using a Perkin-Elmer Optima 5300 V (Galbraith Laboratories, Knoxville, TN). The relaxation rates were then normalized to the resultant concentrations to obtain the relaxivity.

Cyclic Voltammetry. Cyclic voltammograms (CV) of the base substrates and the chelates were recorded using an Autolab PGSTAT30 potentiostat (Utrecht, The Netherlands). A three-electrode system was employed: (i) the reference electrode (Ag/AgCl), (ii) the working electrode (Au), and (iii) a counterelectrode (platinum wire). CV tracings were recorded from 0 to 0.75 V versus the reference electrode at a scan rate of 50 mV/s. The Britton−Robinson (B−R) solution at pH 2 was used as electrolyte.

EPR Measurements. Electron paramagnetic resonance (EPR) measurements were performed at room temperature using a Varian E-line X-band spectrometer (Varian E-122 spectrometer). 2-Methyl-2-nitrosopropane (MNP) was used as the spin-trap. The chelates (5 mM) as well as the MNP (20 mM) were prepared in 50 mM Na_2HPO_4, 100 μM diethylenetriaminepentaacetic acid, pH 8. While avoiding light exposure, the chelate solutions were mixed with MNP followed by MPO (10 U or 50 μg/mL) and H_2O_2 (2 μL of H_2O_2 (3%)) to initiate agent activation.

Simulations of the EPR spectra were performed using the program FIT[22−24] based on the EPRLF engine developed by Schneider et al.[25] and later by Budil et al.[24] to simulate motionally modulated EPR spectra. A two population model was used to simulate the spectra for mono-5HT-DTPA and bis-5HT-DTPA, while a one population model was used to simulate the spectra for bis-*o*-dianisidine-DTPA. The simulations assumed isotropic *g*- and

(18) Nahrendorf, M.; Sosnovik, D.; Chen, J. W.; Panizzi, P.; Figueiredo, J. L.; Aikawa, E.; Libby, P.; Swirski, F. K.; Weissleder, R. *Circulation* **2008**, *117*, 1153–60.
(19) Breckwoldt, M. O.; Chen, J. W.; Stangenberg, L.; Aikawa, E.; Rodriguez, E.; Qiu, S.; Moskowitz, M. A.; Weissleder, R. *Proc. Natl. Acad. Sci. U.S.A.* **2008**, *105*, 18584–9.
(20) Chen, J. W.; Breckwoldt, M. O.; Aikawa, E.; Chiang, G.; Weissleder, R. *Brain* **2008**, *131*, 1123–33.
(21) Querol, M.; Chen, J. W.; Weissleder, R.; Bogdanov, A., Jr. *Org. Lett.* **2005**, *7*, 1719–22.
(22) Wiener, E. C.; Auteri, F. P.; Chen, J. W.; Brechbiel, M. W.; Gansow, O. A.; Schneider, D. J.; Clarkson, R. B.; Lauterbur, P. C. *J. Am. Chem. Soc.* **1996**, *1996*, 7774–7782.
(23) Chen, J. W.; Clarkson, R. B.; Beldford, R. L. *J. Phys. Chem.* **1996**, *100*, 8093–8100.
(24) Chen, J. W.; Auteri, F. P.; Budil, D. E.; Beldford, R. L.; Clarkson, R. B. *J. Phys. Chem.* **1994**, *98*, 13452–13459.
(25) Schneider, D. J.; Freed, J. H. A User's Guide to Slow-Motional ESR Lineshape Calculations. *Biological Magnetic Resonance*; Academic Press: New York, 1989; Vol. 8.

a-values as well as isotropic rotational dynamics, which we believe were reasonable given that MNP is a small molecule and that at room temperature the molecules are at or near the fast-motion regime.

Specific Activity of the Peroxidases. The specific activity of myeloperoxidase and eosinophil peroxidase was determined by UV/vis spectrophotometry on a Varian Cary 50 spectrometer (Palo Alto, CA), using guaiacol, and monitored at 470 nm according to the method of Klebanoff et al.[26]

Enzyme-Mediated Polymerization. Reactions with MPO were carried out at room temperature in the presence of 0.5 mM of the Gd-imaging agents dissolved in phosphate-buffered saline enriched with 5.5 mM of glucose. T_1 relaxation time was measured before MPO addition using an inversion−recovery pulse sequence on the Bruker Minispec (Bruker Analytics, North Bellirica, MA) at 0.47 T (20 MHz) at 40 °C. The reaction was initiated by the addition of an aliquot containing the enzyme (10 U MPO) and 4 μL of glucose oxidase (GOX) (1 mg/mL) because GOX can better mimic hydrogen peroxide production in vivo. Glucose can be oxidized by GOX to glucono-1,5-lactone generating at the same time hydrogen peroxide. To avoid GOX from competing with MPO oxidation of the imaging agents, we optimized the GOX concentration by titration experiments (between 2 and 8 μL @ 1 mg/mL) to obtain the largest change in T_1 before and after MPO was added (data not shown). After 30 min of enzyme incubation, T_1 was measured again. The degree of activation by MPO was expressed as the ratio T_1 (before MPO)/T_1 (after MPO). To test the specificity of the imaging probes to report myeloperoxidase activity, we perform the same measurements in the presence of eosinophil peroxidase instead of MPO.

MALDI-TOF Measurements. MALDI-TOF mass spectrometry was performed using an Applied Biosystems Voyager DE Pro at the Tufts University Core Facility (Boston, MA). The imaging agents (1 mM) were prepared in PBS enriched with 5.5 mM of glucose, and the polymerization was initiated by the addition of an aliquot containing the enzyme (10 U MPO) and 4 μL of glucose oxidase (GOX) (1 mg/mL).

Interactions with Proteins. This experiment was performed to determine possible binding between the activated imaging agents and amino acid residues on the surface of proteins. 0.5 mM of Gd agents was prepared in the presence of a 1 mg/mL polypeptide rich in Tyr (Poly (Glu, Tyr) (1:1)) or in the presence of a 1 mg/mL polypeptide without tyrosine (Poly (Glu, Ala) (6:4)). The T_1 values were measured before and after addition of the MPO using the same conditions described above.

MR Imaging. The MR imaging experiments were performed on a 1.5 T whole body GE Signa scanner (GE Healthcare, Waukesha, WI). For all in vivo MR imaging experiments, precontrast T2- (TR = 2000, TE = 100, ETL = 8, NEX = 4, fast spin echo sequence, acquisition time = 4:57 min) and T1-weighted images (at 1.5 T, TR = 500, TE = 11, NEX = 4, spin echo sequence, acquisition time = 5:59 min) with fat saturation were initially performed to locate the embedded gels. For these experiments, matrix size = 256 × 128, FOV = 10 × 7.5 cm, slice thickness = 1 mm, 22 slices. The images were acquired in the coronal plane. The MPO imaging agents (0.3 mmol/kg) were injected intravenously via the tail vein of the mouse. The mouse was immediately imaged after the injection of the contrast agent using serial fat saturated T_1-weighted sequences (as above for precontrast imaging) for at least 3 h.

MPO/Matrigel Imaging Experiments (n = 13). The protocol for animal experiments was approved by the institutional animal care committee. Nine-week-old C57BL6 male mice were obtained from Jackson Laboratories (Bar Harbor, ME). Matrigel (Beckton−Dikinson, San Jose, CA), a Ewing's sarcoma basement membrane matrix, was used to embed human MPO (Lee Biosolutions, St. Louis, MO). This was chosen to reflect deposits of human MPO in inflamed tissue in a mouse model. 400 μL of a 1:1 mixture of Matrigel and minimal essential medium (Cambrex, East Rutherford, NJ) was injected slowly into the thighs of each mouse 1 h prior to imaging. The right thigh mixture also contained 10−15 U of MPO and 4 μL of glucose oxidase (1 mg/mL), while the left thigh mixture contained no enzyme to serve as an internal control. For the MPO sensitivity experiments, 0.3 mmol/kg of bis-5HT-DTPA-Gd was injected intravenously to monitor MPO activity from 5 to 40 U embedded in Matrigel as described above, and the results were expressed as U of MPO per mg of gel.

Image Analysis. For normalized signal intensity measured on T_1-weighted images, mean ± standard deviation (SD) values were obtained in regions of interest (ROI). Contrast-to-noise ratios (CNR) were computed for each ROI. Within each animal, the CNR values were normalized to the maximum value to compute the relative CNR (rCNR). The analysis was performed using the software OsiriX v3.5 (http://www.osirix-viewer.com/).

Cell Viability Studies. The evaluation of the possible cytotoxic effects for the MPO probes was carried out using NIH 3T3 cells. In parallel to check the possible cytotoxicity of the probes once activated by the MPO, RAW 264.7 cells were used. RAW 264.7 cells can generate MPO in the presence of *E. coli* lipopolysacharide (LPS) (10 μg/mL). Cytotoxicity was evaluated using the 3-(4,5-dimethylthiazol-2-yl)2,5-diphenyl-tetrazoilum bromide (MTT) reduction assay, which measures cell metabolic activity.[27] The Gd agents were dissolved in DMEM plus 10% FBS at the concentrations of 0.025, 0.05, 0.1, 0.25, 0.75, 1, 2.5, and 5 mM. The cells were placed in a 96-well cell culture plate (1.5×10^4 cells/100 μL) and treated with the Gd agents and the controlled medium for 12 h, then incubated with 0.5 mg/mL MTT for 2 h. A lysing buffer that dissolves the blue formazan crystals was added to each well, and the plates were incubated overnight at 37 °C. Optical density was measured at 570 nm, and values were expressed as a percentage of control well values (wells containing cell culture medium without the Gd agents). Oxidative-sensitive dye, 2′7′-dichlorodihydrofluorescein diacetate, DCFH-DA, was used to confirm MPO release through formation of radical generation after LPS activation.[28] For that, RAW 264.7 cells cultured in 96-wells, previously treated with 10 μg/mL of LPS for 3 and 24 h, were labeled with DCFH-DA for 20 min in the dark. The intensity of fluorescence signal emitted by 2′7′-dichlorofluorescein (DCF) due to oxidation of DCFH by cellular ROS was detected using a microplate reader Teca Safire2 (Tecan, Mannedorf, Switzerland) ($\lambda_{excitation}$ = 485 nm, $\lambda_{emission}$ = 530 nm).

Kinetic Stability of the Gd Substrates: Transmetallation. This method reflects the kinetic stability of the Gd^{3+} complexes when competing metal ions such as Zn^{2+} ions, which can displace the Gd^{3+} ion from the chelates, are present. For each reaction, 10 μL of 250 mM of $ZnCl_2$ in water was added to 1 mL of 2.5 mM imaging agents in pH = 7 phosphate buffer. We monitored the evolution of T_1 values of the solutions for 3 days. The results are expressed using two indices: a kinetic index, which is the time required to reach 80% of the initial R_1 value, and a thermodynamic index, which is the $R_1(t = 4320)/R_1(t = 0)$ value measured after 3 days (4320 min).

Results

Redox Characterization of the MPO Imaging Agents. The MPO catalytic center consists of a heme group that can undergo redox reactions described in Scheme 1.

In the presence of H_2O_2, the native enzyme can be oxidized to form the redox intermediate compound I, which can transform halides, particularly Cl^-, into hypochlorous acid, HOCl, a potent antimicrobial oxidant. Compound I is also capable of catalyzing

(26) Klebanoff, S. J.; Waltersdorph, A. M.; Rosen, H. *Methods Enzymol.* **1984**, *105*, 399–403.

(27) Hansen, M. B.; Nielsen, S. E.; Berg, K. *J. Immunol. Methods* **1989**, *119*, 203–10.

(28) Kimura, K.; Ito, S.; Nagino, M.; Isobe, K. *Biochem. Biophys. Res. Commun.* **2008**, *372*, 272–5.

Scheme 1. Myeloperoxidase (MPO) Cycle and Standard Reduction Potential (E°) for Each Part of the Cycle[a]

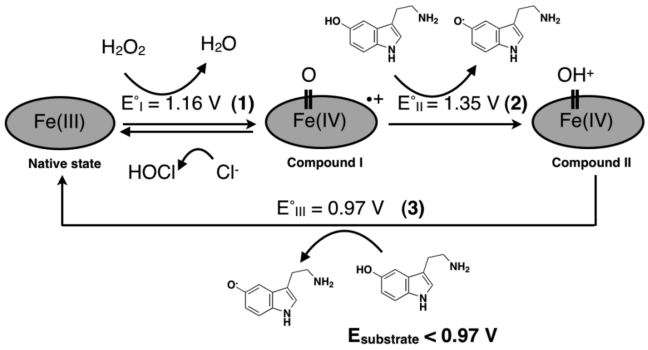

[a] The efficacy of compound II to complete the cycle is key to MPO agent design. For an agent to be a substrate instead of an inhibitor for MPO, $E_{substrate}$ needs to be less than the reduction potential of compound II of 0.97 V.

the oxidation of aromatic substrates like tyrosine or 5-hydroxytryptamine through $1e^-$ oxidation to form compound II, which can itself also oxidize aromatic substrates to recover the native enzyme. The resultant oxidized substrate can form dimers and oligomers. Therefore, to systematically assess whether a given compound is a suitable substrate for MPO, we evaluated the reduction potential of candidate agents. Based on the standard reduction potential relative to the MPO intermediates (compound I/compound II = 1.35 V; compound II/native state = 0.97 V), the recovery of the native enzyme can only take place when the reduction potential of the substrate is lower than 0.97 V (Scheme 1).[29] Therefore, we sought substrates that have reduction potentials less than 0.97 V. We identified the base substrates 4-aminophenol, o-dianisidine, and 5-hydroxytryptamine as potential MPO substrates that, in addition to having a reduction potential <0.97 V, also may be conjugated to DTPA. These substrates demonstrated a significant UV/vis spectral shift upon the addition of MPO and H_2O_2, consistent with MPO-mediated oxidation and oligomerization (data not shown). These substrates were then conjugated to the chelating agent DTPA as potential MR imaging agents (Figure 1).

To determine the reduction potential of the chelates, we performed cyclic voltammetry measurements. The results are shown in Table 1.

To check if the conjugation of the base substrate to the DTPA backbone changes their redox properties, Table 1 also shows the redox properties for the unmodified base substrates. We found no significant change in the reduction potential upon conjugation of the substrates to DTPA, except for bis-4-aminophenol-DTPA, which lost its redox properties once conjugated to DTPA. In this study, we assume that the redox properties of the chelates would not change after complexation to Gd^{3+}.

EPR Measurements Reveal Radical Generation upon Agent Activation by MPO. MPO-mediated dimerization and oligomerization of tyrosine has been found to proceed via free radical formation and $1e^-$ donation to MPO compounds I and II.[30] However, this has not been confirmed for other types of MPO substrates such as indoles and *o*-dianisidine compounds. To determine if these other substrates also undergo radicalization in the presence of MPO, we performed electron paramagnetic resonance (EPR) spin trapping experiments using the spin trap 2-methyl-2-nitrosopropane (MNP). The EPR spectrum for MNP is characterized by a low background three-line spectrum corresponding to the light-induced formation of di-*tert*-butyl-nitroxide (17 G) (Figure 2e).[30]

After the addition of MPO and H_2O_2 to the chelates, we observed an increase in the signal intensity for mono-5HT-DTPA, bis-5HT-DTPA, and bis-*o*-dianisidine, signifying the formation and trapping of free radicals (Figure 2a−c). Control solutions of MNP with MPO and H_2O_2 but without the substrates resembled the baseline MNP spectrum (Supporting Information Figure SI5). A previous EPR study of MPO-tyrosine radical generation showed an a_N of 15.6 G for the MNP-tyrosyl radicals adduct.[30] However, in contrast to the tyrosine EPR spectrum with a single population of $a_N = 15.6$ G, two populations were observed with a_N of 15.1 and 17.1 G for the 5HT compounds (see Figure 2f and g). The a_N of 15.1 G for both mono- and bis-5HT-DTPA confirmed the generation of MNP-5HT radical adducts after MPO activation. The 17.1 G lines likely resulted from the decomposition of MNP, which appeared to be facilitated in the presence of the 5HT groups, because tyrosine and bis-*o*-diansidine-DTPA did not exhibit this. Simulations of the 5HT spectra with a two populations model yielded 49% for mono-5HT-DTPA and 35% for bis-5HT-DTPA for the 15.1 G population. For bis-*o*-dianisidine-DTPA, a single a_N of 15.8 G was observed (Figure 2h). Finally, for bis-4-aminophenol-DTPA, no significant radical formation was observed (Figure 2d), corroborating the cyclic voltammetry results that bis-4-aminophenol-DTPA did not have a detectable redox property. These findings show that bis-4-aminophenol-DTPA cannot be oxidized by MPO and explains the lack of relaxivity change when MPO/H_2O_2 was added to bis-4-aminophenol-DTPA-Gd. Therefore, this agent was not used in the subsequent studies.

In Vitro Relaxometric Characterization of the MPO Imaging Substrates. In vitro characterization of the ability of the gadolinium substrates to report MPO activity was performed using relaxometric methods. In the presence of MPO and hydrogen peroxide, we have shown that these MPO imaging agents can dimerize and oligomerize after being activated by compounds I and II (please also see Supporting Information Figure SI6).[31,32] These changes result in an increase of the agent size with consequent increase in the T_1 relaxivity (Scheme 2).

The mono-5HT-DTPA-Gd complex showed the largest T_1 change after activation, demonstrating that this agent has the highest degree of oligomerization in vitro when activated by MPO (Table 2) (also see Supporting Information Figure SI6a).

Interestingly, the bis-*o*-dianisidine-DTPA-Gd agent showed a small T_1 change after MPO addition as compared to the other two complexes, corroborating the lower degree of the polymerization in vitro seen by MALDI-TOF (see Supporting Information Figure SI6c). Eosinophil peroxidase, EPO, another human peroxidase found in certain inflammatory conditions, was also used to test the polymerization of our imaging agents. Unlike MPO, which causes >1.5-fold T_1 relaxivity change in the agents, the T_1 relaxivity barely changed with EPO for the candidate agents (Table 2). These in vitro findings further corroborated our previous in vivo findings that no agent activation was observed in myocardial infarction and stroke

(29) Furtmuller, P. G.; Arnhold, J.; Jantschko, W.; Pichler, H.; Obinger, C. *Biochem. Biophys. Res. Commun.* **2003**, *301*, 551–7.
(30) McCormick, M. L.; Gaut, J. P.; Lin, T. S.; Britigan, B. E.; Buettner, G. R.; Heinecke, J. W. *J. Biol. Chem.* **1998**, *273*, 32030–7.
(31) Chen, J. W.; Querol Sans, M.; Bogdanov, A., Jr.; Weissleder, R. *Radiology* **2006**, *240*, 473–81.
(32) Querol, M.; Chen, J. W.; Bogdanov, A. A., Jr. *Org. Biomol. Chem.* **2006**, *4*, 1887–95.

MR imaging agents

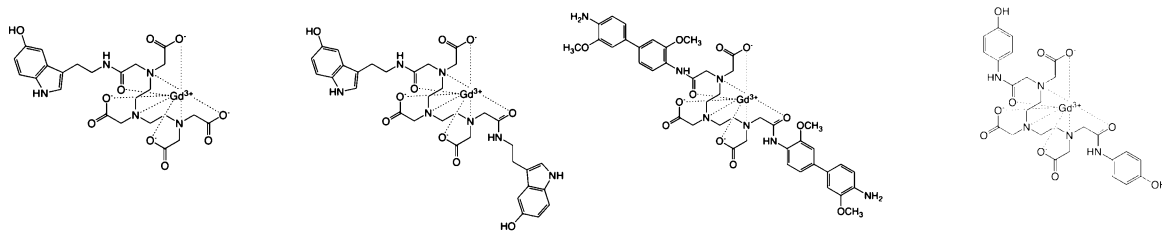

	mono-5HT-DTPA-Gd	bis-5HT-DTPA-Gd	bis-*o*-dianisidine-DTPA-Gd	bis-4-aminophenol-DTPA-Gd
r_1 ($mM^{-1}s^{-1}$)	5.1	5.6	7.3	4.8
Ref.	this study	*a*	this study	this study

Figure 1. MR imaging agents described in this work, based on the DTPA-Gd backbone conjugated with the base substrates (5-hydroxytryptamine (5HT), *o*-dianisidine, and 4-aminophenol). Imaging agents synthesized are: mono-5HT-DTPA-Gd, bis-5HT-DTPA-Gd (*a*, refs 27, 28), bis-*o*-dianisidine-DTPA-Gd, and bis-4-aminophenol-DTPA-Gd. Relaxivity values (mM^{-1} s^{-1}) for each imaging agent are also shown.

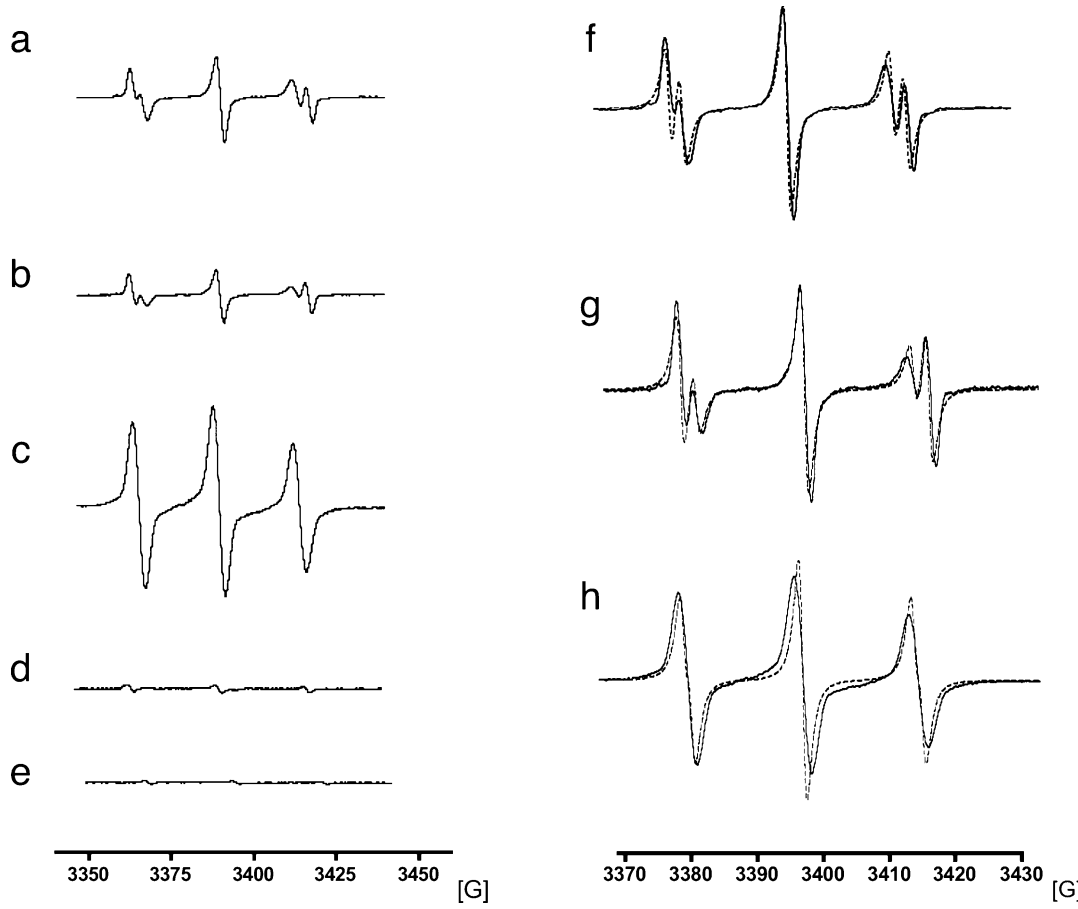

Figure 2. EPR spectra of the radicals generated after MPO−H_2O_2 activation using the 2-methyl-2-nitrosopropane (MNP) as a spin trap. (a) Mono-5HT-DTPA, (b) bis-5HT-DTPA, (c) bis-*o*-dianisidine-DTPA, (d) bis-4-aminophenol-DTPA, (e) MNP only. (f and g) Amplified spectra with simulations to better show the two populations for mono-5HT-DTPA and bis-5HT-DTPA, and (h) the single population for bis-*o*-dianisidine. Chelates were prepared in phosphate solution pH = 8 and activated using MPO (10 U) and H_2O_2 (2 μL of 3% H_2O_2).

Table 1. Reduction Potential (*E*) Measured from Cyclic Voltammetry at 298 K and pH 2 for the Chelates and for Their Parent Base Substrates (Bold)

	5HT	mono-5HT-DTPA	bis-5HT-DTPA	***o*-dianisidine**	bis-*o*-dianisidine-DTPA	**4-aminophenol**	bis-4-aminophenol-DTPA
E(V)	**0.71**	0.62	0.63	**0.57**	0.65	**0.67**	not detectable

Scheme 2. Activation Mechanism of the MR Imaging Agents by the MPO−H_2O_2 System[a]

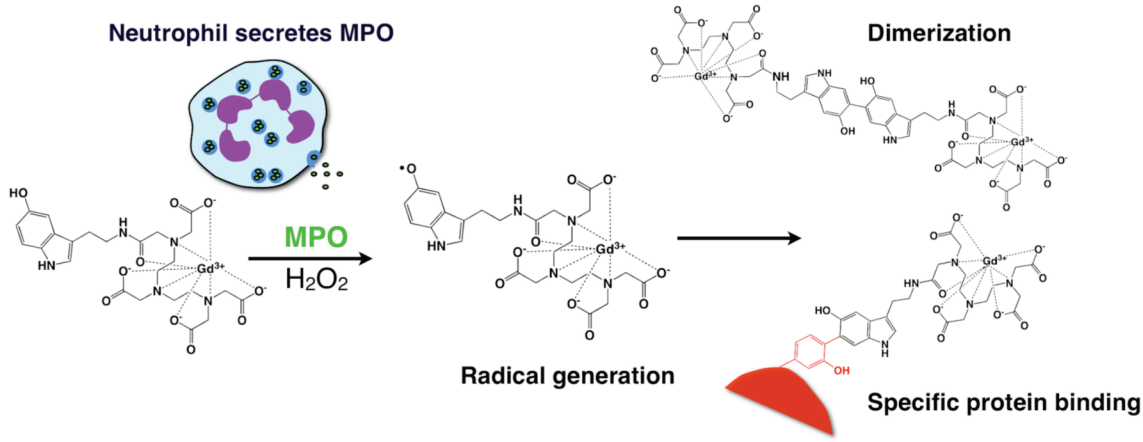

[a] Myeloperoxidase, MPO (green bubbles), is localized in the azurophilic granules (blue bubbles) of the neutrophils. The MPO-sensing moiety conjugated to the gadolinium complex can be oxidized by MPO in the presence of H_2O_2 to result in radical formation. The radicals can form dimers and oligomers with other radicals and can bind to other phenolic residues, such as tyrosine, on the protein surface. Both activation effects result in higher T_1 relaxivity. The binding to proteins can further result in prolonged enhancement of the activated agents.

Table 2. In Vitro Assessment of the MR Imaging Agents Using Relaxometric Measurements (0.47 T)[a]

		T_1 ratios before/after MPO		
buffer solution	human peroxidase	mono-5HT-DTPA-Gd	bis-5HT-DTPA-Gd	bis-*o*-dianisidine-DTPA-Gd
PBS	MPO	1.8	1.7	1.5
PBS	EPO	1.2	1.2	1.0
PBS + polypeptide (Ala−Glu)	MPO	1.8 (0%)	1.7 (0%)	1.5 (0%)
PBS + polypeptide (Tyr−Glu)	MPO	2.2 (22%)	2.7 (59%)	2.1 (40%)

[a] Eosinophil peroxidase (EPO) was also used to test the specificity of the agents. Results obtained are expressed as the ratio (T_1 before MPO)/(T_1 after MPO). We also repeated the same experiments in the presence of either poly(Glu,Tyr) or poly (Glu,Ala) polypeptides.

models using $MPO^{-/-}$ mice with the prototype bis-5HT-DTPA-Gd agent.[18,19] These results confirm specificity of the agents for MPO.

Activated Agents Interact with Proteins Containing Tyrosine. Phenols such as tyrosine have been found to be capable of cross-linking proteins after oxidation by MPO.[31,33] It has not been shown if other species such as indoles and *o*-dianisidine can also cross-link proteins when oxidized by MPO. Furthermore, it is possible that such cross-linking ability may be altered by the chemical modifications needed to conjugate these substrates to a chelating backbone such as DTPA. In these experiments, we found that the imaging agents, when activated by MPO, demonstrated a further increase in relaxivity when exposed to a polypeptide containing tyrosine residues, confirming that they can cross-link proteins (Table 2). However, each agent showed different degrees of relaxivity increase. Both bis agents demonstrated a large increase in relaxivity (>40%), while the mono-5HT-DTPA-Gd agent showed a mild increase in relaxivity (~20%). In contradistinction, no relaxivity change was observed when the agents were activated in the presence of a control peptide that did not contain tyrosine for any of the three imaging agents, confirming that the cross-linking occurs between the activated substrates and the tyrosine residues.

(33) Heinecke, J. W. *Toxicology* **2002**, *177*, 11–22.

MR Imaging Reveals Different in Vivo Behavior for the Agents. To validate the lead agents for in vivo imaging, we performed MR imaging after the injection of the test imaging agents in mice, using Matrigel to embed the MPO in the right thighs of mice. The choice of Matrigel as inflammation model instead of, for instance, *E. coli* LPS injected intramuscularly was due to higher reproducibility of the Matrigel model. All three agents demonstrated a large increase in enhancement (more than 2-fold increase in CNR) in the MPO-containing gel (right) as compared to the control gel (left), consistent with MPO-mediated activation (Figure 3a). In contrast, in a previous study, we performed control experiments using the nonspecific DTPA-Gd that did not demonstrate any increased enhancement in the MPO-containing gel.[31]

Interestingly, as may be predicted from the in vitro results, there were substantial differences in the rate of agent activation and clearance between these agents. The activated mono-5HT-DTPA-Gd reached peak increased T_1-weighted enhancement during the first hour of imaging and was cleared at nearly the same rate as the parent, nonactivated agents. For the activated bis-5HT-DTPA-Gd, the peak occurred at around 90 min after agent administration, and there was a slower clearance rate as compared to that of the control site. The activated form of bis-*o*-dianisidine-DTPA-Gd, interestingly, did not seem to be clearing within the experimental time frame of 3 h and continued to show an increase in enhancement over time.

To evaluate the sensitivity of the agents for different concentrations of MPO, we varied the amount of MPO embedded in the gels and imaged these mice using the same dose of bis-5HT-DTPA-Gd. Over the range of MPO concentrations we tested, we found that the enhancement for bis-5HT-DTPA-Gd was linearly proportional to MPO concentration (Figure 3b) and was able to detect an MPO concentration as low as 0.005 U/mg of gel. This would allow sensitive detection of MPO activity at the earliest stages of inflammation (e.g., in a murine stroke model, the MPO level was 0.15 U/mg 1 day after stroke induction).[19]

Kinetic Stability of the Gadolinium Complexes. One method to assess the stability of the gadolinium complexes is to measure the degree of transmetallation in the presence of another

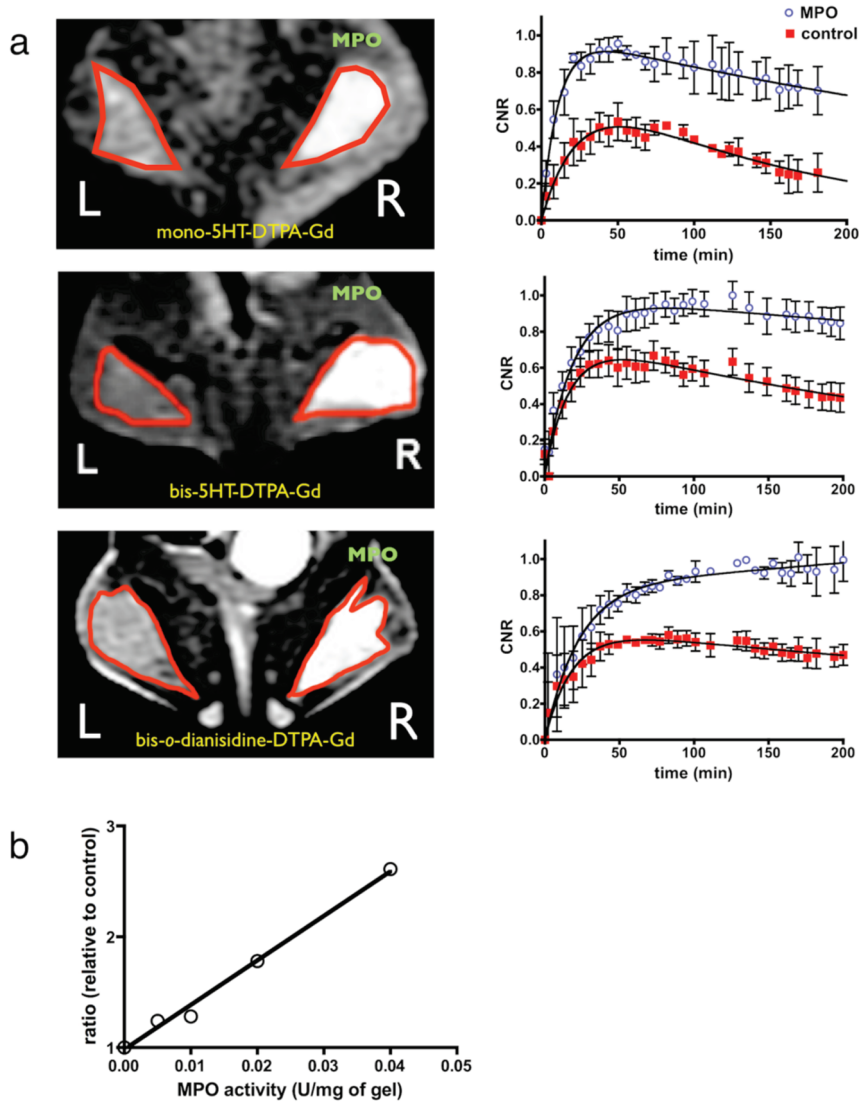

Figure 3. (a) In vivo assessment of the agents mono-5HT-DTPA-Gd, bis-5HT-DTPA-Gd (data taken from ref 31), and bis-*o*-dianisidine-DTPA-Gd as MPO activity reporters. The right side (R) contained human MPO and glucose oxidase embedded in Matrigel. The left side (L) contains only Matrigel and medium. All three agents were able to identify areas of MPO activity. The line graphs illustrate the evolution of contrast-to-noise ratios (CNR) for each imaging agent in the presence of MPO versus control, demonstrating striking differences in the pharmacokinetics of each activated agent from the nonactivated parent agent as well as from the other agents. (b) Sensitivity of the bis-5HT-DTPA-Gd agent to report MPO concentrations in vivo.

competing metal.[34] Zn^{2+} is a good competing metal ion because it is present in high concentration in blood (55−125 μmol/L) and because it has an affinity to DTPA similar to that of Gd^{3+}.[34] Because the displacement of Gd^{3+} by Zn^{2+} will result in a decrease in the T_1 relaxation rate (R_1) due the precipitation of the Gd^{3+} ions in phosphate buffer as $Gd(PO_4)$, the effect of the transmetallation can be evaluated through two parameters: a kinetic index given by the time required to lose 20% of the initial R_1 value and a thermodynamic index, which is the percentage of R_1 after 3 days as compared to the initial value (see Supporting Information Figure SI7). From both indices, the imaging agents modified with 5HT were similar to or better than that observed for the clinical, conventional agent DTPA-Gd, especially the bis-version of the agent, suggesting that Gd^{3+} metal center is not easily displaced by competing Zn^{2+} ions (Table 3). However, the bis-*o*-dianisidine-DTPA-Gd complex demonstrated substantially lower transmetallation indices, suggesting the Gd^{3+} in this complex could be more easily displaced by the Zn^{2+} ions.

Table 3. Zinc Transmetallation Kinetic Stability of Gd^{3+} of the Imaging Agents in the Presence of Equimolar Zn^{2+} (2.5 mM)[a]

	$R_1(t = 4320)/R_1(t = 0)$	t for $R_1(t)/R_1(t = 0) = 0.8$
bis-5HT-DTPA-Gd	0.76	2866
mono-5HT-DTPA-Gd	0.48	367
bis-*o*-dianisidine-DTPA-Gd	0.25	67
DTPA-Gd	0.56	250
BMA-DTPA-Gd	0.09	50−60[b]

[a] Relaxation rate (R_1) (s^{-1}) was monitored for 3 days (t reported in min) at 40 °C. Results are expressed by two indexes: kinetic index ($R_1(t)/R_1(t = 0) = 0.8$) and a thermodynamic index ($R_1(t = 4320)/R_1(t = 0)$). [b] Data taken from ref 34.

Cytotoxicity. To evaluate the possible toxic effects of the Gd-based complexes, we evaluated the cytoxicity in the NIH 3T3 cell line (Figure 4a).[27] There was no significant toxicity effect up to 5 mM for the bis-5HT-DTPA-Gd agent and for the mono-5HT-DTPA-Gd, well above the expected in vivo concentration.

(34) Laurent, S.; Elst, L. V.; Copoix, F.; Muller, R. N. *Invest. Radiol.* **2001**, *36*, 115–22.

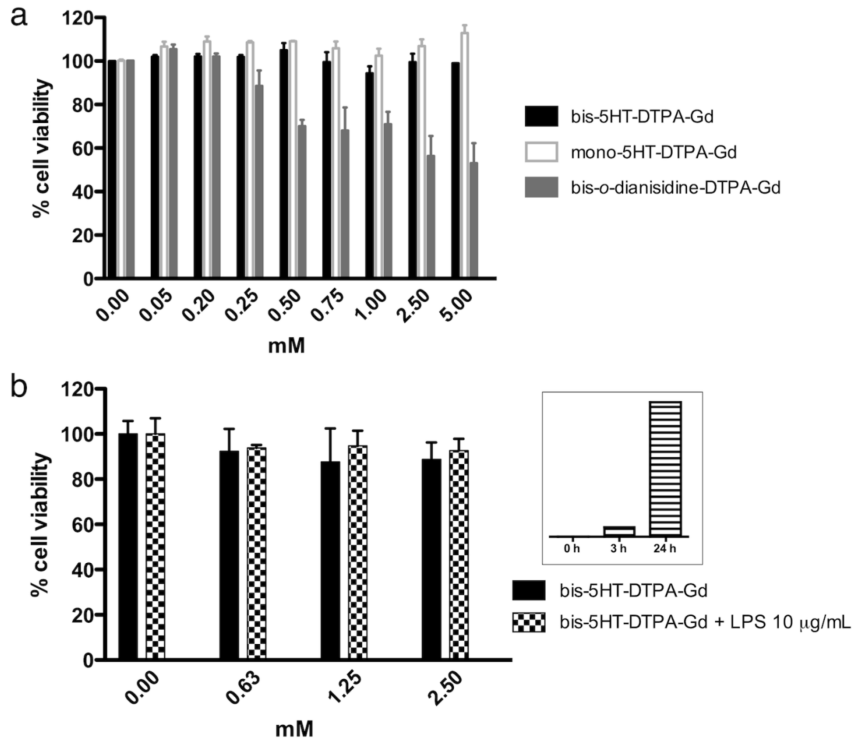

Figure 4. (a) Cell viability of NIH 3T3 cells in the presence of mono-5HT-DTPA-Gd (gray open), bis-5HT-DTPA-Gd (black filled), and bis-*o*-dianisidine-DTPA-Gd (gray filled) evaluated using the MTT assay. (b) Cell viability of quiescent RAW cells in the presence of bis-5HT-DTPA-Gd (black filled) was not significantly altered when the RAW cells were activated with 10 μg/mL of LPS (square filled), evaluated using the MTT assay. Confirmation of RAW cell activation was confirmed by the detection of ROS species using the DCFH-DA dye after LPS activation (inset).

However, as can be predicted from the zinc transmetallation study, the bis-*o*-dianisidine-DTPA-Gd agent demonstrated substantial toxic effect at 0.3 mM (<80% viable cells), with <50% viable cells at 5 mM. To further evaluate if the activation of the agents would cause additional toxicity, we also studied the toxicity in macrophages (RAW cells) with and without incubation with LPS to activate the macrophages. Upon stimulation by LPS, the RAW cells would secrete MPO to activate the MPO substrates.[35] To confirm activation of the macrophages under this experimental condition, we measured radical generation using the DCFH-DA dye (inset, Figure 4b). We found no difference in viability (Figure 4b) between the activated cells and the nonactivated cells for bis-5HT-DTPA-Gd, consistent with that the activated MPO imaging agents do not present additional cytotoxicity effects.

Discussion

In this study, we showed that MPO oxidation leads to radicalization of the imaging agents. These intermediate compounds can combine to form dimers and oligomers as well as cross-link proteins containing tyrosine residues. These MPO-mediated changes increase the molecular size and consequent shortening of T_1, resulting in >2-fold increased T_1-weighted enhancement on in vivo imaging relative to agents that are not activated. We have identified that the reduction potential (<0.97 V to allow the recovery of the native form of the MPO) of the base substrates (5HT, *o*-dianisidine, and 4-aminophenol) after conjugation to a chelating backbone is an important indicator of whether the conjugated substrate could be activated by MPO. We also demonstrated in this and previous studies that only MPO, but not EPO, can highly activate these agents to report enzyme activity in vitro and in vivo. Furthermore, using a 5HT-based agent, we showed high sensitivity of the agents for MPO activity as low as 0.005 U/mg.

We found that one of the chelates, bis-4-aminophenol-DTPA, despite having a suitable reduction potential prior to DTPA conjugation, cannot be oxidized by MPO. This was because the conjugation of the base substrates to DTPA occurs through an amide bond, which is a strong electron-withdrawing group, resulting in the subtraction of the electron density from the aromatic moiety.[36] This amide bond is directly attached to the phenolic group, whereas for the other imaging agents, this electron-withdrawing group is far enough to not disturb the electron density of the aromatic moieties. Design of future optimized imaging agents needs to take into account that conjugated base substrates (chelates) with strong electron-withdrawing groups may not be polymerized by MPO because of the loss of the reduction redox potential.

We found that mono-5HT-DTPA-Gd demonstrated the highest increase in relaxivity in vitro as well as the highest degree of oligomerization. The extent of oligomerization is likely related to the accessibility of the probe to the active site of the enzyme. The conjugation of aromatic phenolic compounds to DTPA increases steric hindrance that can diminish interactions with the MPO active site. Thus, the monosubstituted agent, being smaller, is able to better reach the active site, consistent with this agent having the highest degree of polymerization (Figure SI6a). Interestingly, while bis-*o*-dianisidine-DTPA generated the highest amount of radicals (Figure 2c), this substrate yielded very little change in T_1 upon activation by MPO in vitro. Because in vitro the relaxivity increase is mainly due to size

(35) Cuschieri, J.; Maier, R. V. *Antioxid. Redox Signal* **2007**, *9*, 1485–97.

(36) Xu, Y. P.; Huang, G. L.; Yu, Y. T. *Biotechnol. Bioeng.* **1995**, *47*, 117–9.

increase, the larger and floppier conformation of the *o*-dianisidine agent may prevent optimal interaction with MPO to generate larger oligomers. This result confirms that, in addition to the redox properties, substrate oxidation by MPO is governed by structural and topological characteristics. The in vitro efficiency of MPO-mediated activation of the mono-5HT-DTPA-Gd is verified in vivo (Figure 3a) where mono-5HT-DTPA-Gd is the agent that is the earliest to peak, consistent with fast interactions with MPO.

Another contribution that affects in vivo image enhancement is protein binding. The mono-5HT agent demonstrated the smallest increase in the T_1 ratio in the presence of poly(Glu, Tyr) as compared to the bis-5HT version, suggesting that a bis-conformation facilitates protein binding to result in higher relaxivities, likely by offering an additional moiety for MPO oxidation. Interestingly, the bis-*o*-dianisidine-DTPA-Gd agent, which in the absence of peptides showed the weakest activation by MPO likely due to its larger size, showed high relative increase in relaxivity in the presence of poly(Glu, Tyr). This finding is corroborated in vivo as this agent showed a large increase in CNR at later time point and did not show substantial clearance over 3 h, consistent with that most of its in vivo efficacy is derived from binding of the activated agent to proteins.

In light of the recent evidence linking nephrogenic systemic fibrosis (NSF) with the presence of free Gd^{3+} in renal failure patients, we chose to evaluate the stability of the agents using a transmetallation method, which evaluates the kinetic lability of the Gd^{3+} ion when other competing metal ions such as Zn^{2+} are also present at physiological conditions. Our results showed that the 5HT-based imaging agents were similar to or even better than DTPA-Gd in Gd kinetic lability. On the other hand, bis-*o*-dianisidine-DTPA-Gd complex was found to be very susceptible to transmetallation, with transmetallation indices similar to Omniscan, the agent most commonly associated with NSF. This increased Gd kinetic lability may be caused by the noncoplanar conformation of *o*-dianisidine, which could allow increased access of Zn^{2+} to the chelate, whereas in 5HT the indolic rings are in a more rigid coplanar conformation, increasing steric hindrance. The very slow clearance of the *o*-dianisidine agent could further increase its in vivo toxicity. However, as its parent base substrate, *o*-dianisidine (3,3′-dimethoxybenzidine), is used in in vitro assay kits to report MPO activity, bis-*o*-dianisidine-DTPA-Gd could be used to screen MPO activity in biological samples in vitro using relaxometric methods.[37,38] On the other hand, for the 5HT-based agents, no cytotoxicity was identified at doses likely exceeding in vivo levels of the agent (estimated to be $\ll$1 mM) using either the parent or the activated agents, suggesting a safe profile for translation to preclinical and clinical studies. Because these agents are based on the DTPA backbone, it is expected that most of the agents will be cleared predominantly by the kidneys and liver, similar to DTPA-Gd. Indeed, in a biodistribution study for bis-5HT-DTPA, we found >90% of the radiolabeled agents to be cleared within 6 h, with the remaining agents found primarily in the liver, kidneys, spleen, and bowel.[31] For activated agents, in a study on mouse experimental autoimmune encephalomyelitis using bis-5HT-DTPA-Gd, we found no evidence of residual enhancement 6 h after agent injection in the diseased organ, suggesting that the binding of activated agents to proteins is reversible and likely cleaved by proteases that are present abundantly in inflamed tissues.[20]

The MPO levels found in human pathological conditions are significantly higher than the MPO concentrations ($\sim$0.05 U/mg) used for this work (e.g., in carotid plaques, MPO has been found to be $\sim$250 U/mg),[38] and should be readily assessed by the imaging agents described here to detect early, presymptomatic disease. This, together with the increased signal observed once these agents are activated, likely will allow much lower doses to be used in translational studies to further improve the safety profile. Future optimization of the MPO agents could use a macrocyclic backbone instead of DTPA to further improve the Gd kinetic lability. In addition, these chelates are readily complexed to radioisotopes, for example, ^{111}In, to convert into nuclear imaging agents that can be used at trace doses.[31]

Conclusions

We identified two new candidate MPO-sensitive imaging agents, in addition to our previously reported prototype agent. Each of these agents possesses a unique activation profile, with different degrees of oligomerization and protein cross-linking capabilities. All three agents were efficacious at identifying sites of MPO activity in vivo. Most of the increased enhancement observed for the mono-5HT-DTPA-Gd agent is from radical formation and subsequent oligomerization, while for the bis-*o*-dianisidine-DTPA-Gd agent the increased enhancement was found to be from protein cross-linking, resulting in significantly delayed clearance of the activated agent. These two agents represent near extremes in the activation mechanism. For bis-5HT-DTPA-Gd, the increased enhancement is from both moderate oligomerization and substantial protein cross-linking, causing slower clearance of the activated agents. Moreover, we observed that the activated agents are cleared from mice within 4−6 h[20] and less than 24 h in rabbits,[39] likely from cleavage by proteases that are abundant at inflamed sites. The differential clearance rates of the activated versus nonactivated bis-5HT-DTPA-Gd agent allow for confirmation of MPO activity at a slightly delayed imaging time point, when the nonactivated agents are mostly cleared from the tissues. On the other hand, mono-5HT-DTPA-Gd may represent an attractive agent in applications where faster diagnosis is required. As MPO is implicated in many prevalent diseases such as atherosclerosis, stroke, and multiple sclerosis, the unique properties identified in this study for each prototype agent could be exploited for different in vitro and in vivo environments and applications. Therefore, future rational development and translation of these MPO-sensitive and other bioactivatable MR imaging agents[40−43] holds promise in bringing biological functional information to MR imaging.

Acknowledgment. We thank Ben Bautz, Alexy Chudnovsky, Martin Etzrodt, and Christopher N. LaFratta for experimental assistance and Brian Rutt for helpful discussions. We also acknowledge Alexei Bogdanov and Manel Querol for early

(37) Spalteholz, H.; Furtmuller, P. G.; Jakopitsch, C.; Obinger, C.; Schewe, T.; Sies, H.; Arnhold, J. *Biochem. Biophys. Res. Commun.* **2008**, *371*, 810–3.
(38) Daugherty, A.; Dunn, J. L.; Rateri, D. L.; Heinecke, J. W. *J. Clin. Invest.* **1994**, *94*, 437–44.
(39) Ronald, J. A.; Chen, J. W.; Chen, Y.; Hamilton, A. M.; Rodriguez, E.; Reynolds, F.; Hegele, R. A.; Rogers, K. A.; Querol, M.; Bogdanov, A.; WeisslederR.; Rutt, B. K. *Circulation* **2009**, *120*, 592–599.
(40) Major, J. L.; Boiteau, R. M.; Meade, T. J. *Inorg. Chem.* **2008**, *47*, 10788–95.
(41) Major, J. L.; Meade, T. J. *Acc. Chem. Res.* **2009**, *42*, 893–903.
(42) Major, J. L.; Parigi, G.; Luchinat, C.; Meade, T. J. *Proc. Natl. Acad. Sci. U.S.A.* **2007**, *104*, 13881–6.

contributions to the development of MPO sensing agents. E.R. was supported by the EC-Marie Curie grant OIF (Molecular Imaging 39639). This work was supported in part by National Institutes of Health Grants KO8HL081170 (J.W.C.) and RO1-HL078641 (R.W.).

(43) Delli Castelli, D.; Terreno, E.; Carrera, C.; Giovenzana, G. B.; Mazzon, R.; Rollet, S.; Visigalli, M.; Aime, S. *Inorg. Chem.* **2008**, *47*, 2928–30.

Supporting Information Available: ^{1}H NMR and mass spectra of chelates; HPLC and mass spectra of the imaging agents; EPR spectra of control solutions; MALDI-TOF mass spectra of imaging agents after MPO activation; and zinc transmetallation profiles of the imaging agents. This material is available free of charge via the Internet at http://pubs.acs.org.

JA905274F